Experimental investigation of the role of shell structure in quasifission mass distributions

D. J. Hinde,[*] R. du Rietz,[†] D. Y. Jeung, K. J. Cook, M. Dasgupta, E. C. Simpson, R. G. Thomas,[‡] M. Evers,[§] C. J. Lin,[¶] D. H. Luong,[‖] L. R. Gasques,[**] R. Rafiei,[††] and A. Wakhle[‡‡]
Department of Nuclear Physics and Accelerator Applications, Research School of Physics, Australian National University, Canberra, ACT 2601, Australia

C. Simenel
Department of Nuclear Physics and Accelerator Applications, Research School of Physics, Australian National University, Canberra, ACT 2601, Australia and Department of Theoretical Physics, Research School of Physics, Australian National University, Canberra, ACT 2601, Australia

(Received 26 September 2022; accepted 9 December 2022; published 29 December 2022)

Background: To understand superheavy element synthesis reactions, quantifying the role of quantum shells in quasifission dynamics is important. In reactions with actinide nuclides, a wide peak in the binary quasifission mass yield is seen, centered close to the ^{208}Pb mass. It is generally attributed to the ^{208}Pb spherical closed shells causing a valley in the potential-energy surface, attracting flux to these mass splits. However, an early experiment studying ^{48}Ca, ^{50}Ti + ^{238}U reactions showed strong evidence that sequential fission plays an important role in generating the observed peak. These conflicting interpretations have not been resolved up to now.
Purpose: This work aims to measure quasifission mass spectra for reactions with nuclei lighter than ^{208}Pb, having negligible sequential fission, to search for systematic features correlated with the proton shells known to affect low-energy fission mass distributions of the same actinide elements.
Methods: Systematic measurements have been made at energies near and below the capture barriers (where quasifission is most prominent) of mass-angle distributions for fission following collisions of ^{48}Ti projectiles with even-even nuclides from ^{154}Sm to ^{200}Hg. Mean excitation energies above the ground-states ranged from 51 to 33 MeV, respectively.
Results: With increasing compound nucleus atomic number Z_{CN}, a rapid transition occurs from fission having characteristics of fusion-fission to fast quasifission. The heaviest reactions form ^{240}Cf, ^{244}Fm, and ^{248}No. Low-energy fission of neighboring isotopes is mass asymmetric, correlated with proton number $Z = 56$. However, peak quasifission yields are at mass-symmetry for all reactions. There appears to be a very small ($\approx$3%) systematic excess of yield correlated with $Z = 56$, however this is at the limit of sensitivity of the experiment.
Conclusions: No significant (>3%) systematic features are seen in the quasifission mass spectra that can be unambiguously identified as resulting from shells. This small influence may result from attenuation of shell effects due to the excitation energy introduced, even in these near-barrier reactions giving low excitation energies typical of superheavy element synthesis reactions.

DOI: 10.1103/PhysRevC.106.064614

I. INTRODUCTION

Quantum shells play a key role in the physics of the heaviest elements. Liquid drop model calculations show that nuclei with $Z \gtrsim 104$ have such low fission barriers that they would be ineffective in preventing fission [1]. Thus, fission would occur before atomic electron shells could be established ($\approx 10^{-14}$ s), and such chemical elements could not be synthesized. Nevertheless, superheavy elements with Z up to 118 have been created in the laboratory [2–7] with lifetimes up to seconds. Their existence results from shell effects at the ground-state that increase the height of the fission barrier, thus providing stability beyond the classical liquid drop model limits.

Cross sections for the synthesis of superheavy elements can be very small ($\approx 10^{-36}$ cm^2) because of the method that

[*]david.hinde@anu.edu.au
[†]Permanent address: Department of Materials Science and Applied Mathematics, Malmö University, S-20506 Malmö, Sweden.
[‡]Present address: Bhabha Atomic Research Centre, Mumbai, India.
[§]Present address: PwC Canberra, Forrest, ACT 2603, Australia.
[¶]Permanent address: China Institute of Atomic Energy, P.O. Box 275(10), Beijing 102413, China.
[‖]Present address: 10 Quinn St., Deer Park, VIC 3023, Australia.
[**]Present address: Universidade de São Paulo, Instituto de Física, Rua do Matao 1371, 05308-090 São Paulo, SP, Brazil.
[††]Present address: Reformulate Health, Woolahra, NSW 2025, Australia.
[‡‡]Present address: Adaptas Solutions, Sydney, NSW, Australia.

must be used for their synthesis. This is in reactions of two massive nuclei, whose large Coulomb repulsion inhibits the desired fusion process. Following contact of the two colliding nuclei, the system generally reseparates through two fast nonequilibrium processes. The fastest is so-called deep-inelastic collisions (abbreviated as DIC), resulting in partial to full energy dissipation but limited mass flow. The second, slower, process is known as quasifission [8–11]. It produces fragments having essentially fully damped kinetic energies, with masses between those of the projectile and target nuclei.

A. Effects of shells in heavy element synthesis reactions

The effect of shell structures appears to be important in the *formation* of superheavy elements [10,11], as well for their existence and properties. Theoretical ideas [12] and experiments [13–17] suggest that collisions of nuclei with multiple closed shells result in smaller quasifission probabilities, and thus higher probabilities of fusion forming heavy elements. This may be correlated with reduced energy dissipation in the initial stages of the collision, perhaps associated with a lower density of single-particle levels near the Fermi surface. The favorable doubly magic neutron-rich nucleus ^{48}Ca has been used to discover all the heaviest elements, with $Z =$ 114 to 118. The current lack of target materials of elements heavier then Cf ($Z = 98$) means heavier beams must be used to create still heavier elements, where DIC and quasifission competition is expected to be much more severe [17–21]. A quantitative understanding is still lacking, compromising reliable prediction of superheavy element cross sections.

Shell effects encountered after energy dissipation, during the quasifission process, have long been postulated to play a significant role in superheavy element synthesis reaction outcomes [22–26]. Shell gaps can result in valleys in the potential-energy surface (PES), which could intercept flux [27–29] that might otherwise lead to fusion, resulting instead in quasifission and thus reducing the fusion probability.

B. Differences between effects of shell structure in fission and quasifission

Shell valleys are known to play a key role in low-energy fission of actinide nuclei, resulting in predominantly mass-asymmetric fission, as described in a recent review on fission [30]. In such low-energy fission from the compact ground-state shape, the valleys are entered *after* passing over the (compact) fission barriers leading to the valleys. The effect of the valleys in general is to attract the system away from the mass-symmetric splits favored by the macroscopic (liquid drop model) potential-energy surface (PES).

In quasifission, the situation is different [29]. In a heavy-ion collision, full energy dissipation is expected to occur soon after contact and therefore at elongated shapes well outside the fission barrier. From this entry point, the system may be pictured as undergoing a random walk (diffusion) over the PES [31,32] from the initial elongated mass-asymmetric (dinuclear) shape. Trajectory fluctuations may take the system to a configuration more compact than the fission barrier, resulting in fusion. However, shell valleys in the PES that lead to scission may intercept and redirect the flux, resulting in more rapid quasifission.

The different entry point into the PES in heavy-ion reactions (close to the mass asymmetry of the entrance channel) also leads to the possibility that shell valleys far from mass symmetry, high on the side of the wide liquid drop potential valley, may also affect quasifission [33]. These may not be evident in low-energy fission from the equilibrium deformation. The different entry point may also increase the effect of the "standard" mass-asymmetric shells, since they must be encountered on the path to mass symmetry. The most prominent shell effect expected to play a role in quasifission reactions involving reactions with actinide nuclides arises from the mass-asymmetric valley in the PES that results from the ^{208}Pb spherical closed shells. This fission mode has not yet been seen so far experimentally in measurements of fission, although the influence of the Pb shells is seen in cluster decay [34].

In quasifission, measured mass distributions for reactions of heavy nuclei with actinide nuclides are dominated by a strong peak close to ^{208}Pb [24,25,28,35–40]. For decades this has been attributed to the effect on the PES of the ^{208}Pb closed shells. This interpretation of experimental results has been supported by many model calculations. Classical Langevin model [31,41–44] calculations of diffusion over a potential-energy surface (PES) having a valley due to ^{208}Pb closed shells [44] produce a peak at quasifission mass-splits corresponding closely to ^{208}Pb. Microscopic time-dependent Hartree Fock (TDHF) calculations predict the most likely binary fragment mass splits. In reactions involving actinide nuclei, these often result in fragments close to ^{208}Pb [29,45], most prominently in collisions with the tips of the deformed actinide nuclei [45]. Other shells have been predicted to similarly affect quasifission [29,46].

The peak in binary quasifission mass splits near ^{208}Pb was initially observed in the 1970s [47] and 1980s [48]. At that time the role of sequential fission of quasifission fragments heavier than ^{208}Pb was discussed [47], and experimental evidence was presented suggesting [48] it should play an important role in generating the peak. This process would convert highly mass-asymmetric binary quasifission events into three-body events, which are rejected in a two-body kinematic coincidence analysis. However, a later influential experimental paper [9] suggested that sequential fission for reactions involving ^{238}U plays a minor role. This conclusion seems to have prevailed subsequently in interpreting quasifission measurements in reactions with all actinide nuclides [24,25,28,36,37,39,45,49].

These two conflicting interpretations have not yet been resolved experimentally. It may well be that both mechanisms play a role, but to disentangle them in reactions with actinide nuclei is difficult.

C. Need for a new approach to investigate shell effects on quasifission mass distributions

The ambiguity arising from the possible role of sequential fission is addressed in this work. Instead of studying reactions with fissile actinide nuclides, here we search for the effects

of shell structure on quasifission dynamics for reactions with target nuclei lighter than ^{208}Pb, where the probability of sequential fission is expected to be negligible. Furthermore, by forming actinide compound nuclei, the role of shell structures in the mass distributions of low energy compound nucleus fission decay is well established. In summary, the idea is to investigate how the well-established shell structure that results in the low-energy mass-asymmetric fission of actinide nuclei affects the quasifission occurring in heavy-ion reactions forming the same elements.

In actinide fission, proton shells around $Z = 54$ in the nascent heavy fragment are found empirically [50,51] to be the main drivers for the mass asymmetry seen at low excitation energies. Thus as the atomic number of the fissioning actinide nuclide increases towards $Z \approx 108$, any features in the mass spectrum due to these shells should move systematically towards mass symmetry, which is indeed observed experimentally [30]. Therefore, to obtain the clearest insight into the role of shell valleys in quasifission dynamics, a systematic investigation of quasifission mass distributions forming a range of actinide elements will be optimal.

The intended compound nucleus masses (actinides) and the requirement that the reactions proceed dominantly by quasifission constrains the choice of reactions to use. The systematic survey by du Rietz *et al.* [20] of quasifission outcomes and timescales for a very wide range of reactions, and the investigation of mass widths for a series of ^{48}Ti-induced reactions by Lin *et al.* [52], indicate that reactions with Ti beams should be well suited.

II. EXPERIMENTAL DETAILS

To carry out the systematic measurements, pulsed beams ($\simeq$1.5 ns FWHM) of ^{48}Ti in the energy range 198–245 MeV were provided by the ANU 14UD tandem electrostatic accelerator, operating at voltages close to 15 MV. The beams bombarded isotopically enriched targets of an isotope of each even-Z element from Sm to Hg (excepting Gd), namely, ^{154}Sm, ^{162}Dy, ^{170}Er, ^{174}Yb, ^{186}W, ^{192}Os, ^{196}Pt, and ^{200}Hg. Measurements included beam energies E with respect to the calculated [53] mean capture barriers energies V_B in the range $E/V_B = 0.98$ to 1.05. Low E/V_B preferentially results in the formation of elongated systems after contact in reactions with the deformation-aligned target nuclei, increasing the probability of quasifission [35,54–58]. It also minimizes excitation energies, thus the influence of the shell valleys should be maximized. Hence the interpretation of the experimental mass distributions focused on data from $E/V_B = 0.98$ to 1.03.

Measured target thicknesses were generally between 15 μg/cm^2 and 170 μg/cm^2, evaporated onto $\approx$20 μg/cm^2 C backings (facing downstream). Only the ^{196}Pt target was self-supporting, of thickness 220 μg/cm^2. Effects of fission fragment and beam particle energy loss in the targets were accounted for iteratively, event-by-event. The target normals were angled at 60° to the beam axis, to minimize energy losses of the fission fragments. Binary events were measured in two 28 cm × 36 cm position-sensitive multiwire proportional counters (MWPCs) [20,59]. They were located on opposite sides of the beam axis, with the normal to the MWPC central timing foils being 18 cm from the target. The resulting scattering angle coverage was 5°–80° and 50°–125°. This enabled full efficiency detection of all fragment pairs with masses from the projectile to the target, for center-of-mass angles ($\theta_{\text{c.m.}}$) between 40° and 140°.

III. EXPERIMENTAL RESULTS AND ANALYSIS

A. Mass-angle distributions

The large angular acceptance and the position sensitivity of the multiwire proportional counters, combined with measurements of time-of-flight of the two fragments, allowed mass-angle distributions (MADs) to be obtained, as detailed in Refs. [20,35,60,61]. The fission mass-ratio M_R at scission—the mass of one fragment divided by the total mass—was determined event-by-event from the ratio of the two fragment velocities in the center-of-mass frame [59].

The azimuthal coverage of the backward angle (trigger) MWPC was 70° for all but the extreme scattering angles, thus the number of events observed is proportional to $d\sigma/d\theta_{\text{c.m.}}$. This means that an angular distribution with $d\sigma/d\Omega$ proportional to $1/\sin\theta_{\text{c.m.}}$ should show a yield in $d\sigma/d\theta_{\text{c.m.}}$ independent of angle. Representative MADs from single beam energies (values of E/V_B are indicated in each panel in Fig. 1 in brackets) are shown in Fig. 1, including all reactions with targets heavier than ^{178}Hf. MADs selected for presentation here are those from the higher E/V_B, since the quasifission cross section increases with E, so the statistics are greater than for measurements at lower energies. These MADs provide an overview of the dynamics of the reactions and will be discussed before the one-dimensional mass-ratio spectra, including data from lower energies, are presented.

The intense bands near $M_R \approx 0.2$ and 0.8 correspond to quasielastic collisions, with little mass deviation from the entrance channel values. Fission and quasifission events lie between them. For the ^{154}Sm target, the fission events show a narrow distribution, centered on mass symmetry at all angles (within experimental uncertainty). Having no significant mass-angle correlation, this is consistent with fusion-fission. In the low-intensity region at $0.3 < M_R < 0.35$, the yield rises at forward angles, signifying a small contribution of quasifission here, consistent with results [62] for ^{48}Ca + ^{154}Sm. In contrast with ^{154}Sm, for ^{200}Hg there is a strong mass-angle correlation, with the highest values of $d^2\sigma/d\theta dM_R$ around $M_R = 0.35$ and $\theta_{\text{c.m.}} = 45°$. For fast quasifission the angular distribution is not constrained [9,28,63,64] to the family of equilibrium angular distributions expected for fusion-fission [65]. Instead it is determined by the distributions of sticking times and angular velocities [9,20,64], which have recently been shown experimentally to be correlated [66]. The strong mass-angle correlation of the quasifission signifies a short reaction time of $\approx 10^{-20}$ s [20,67], corresponding to *fast* quasifission according to Ref. [40].

For targets intermediate in mass and atomic number between ^{154}Sm and ^{200}Hg, the MADs show a smooth transition between these two extreme outcomes. In particular, the ^{164}Dy reaction appears to consist of an underlying quasifission component (having a mass-angle correlation), and a

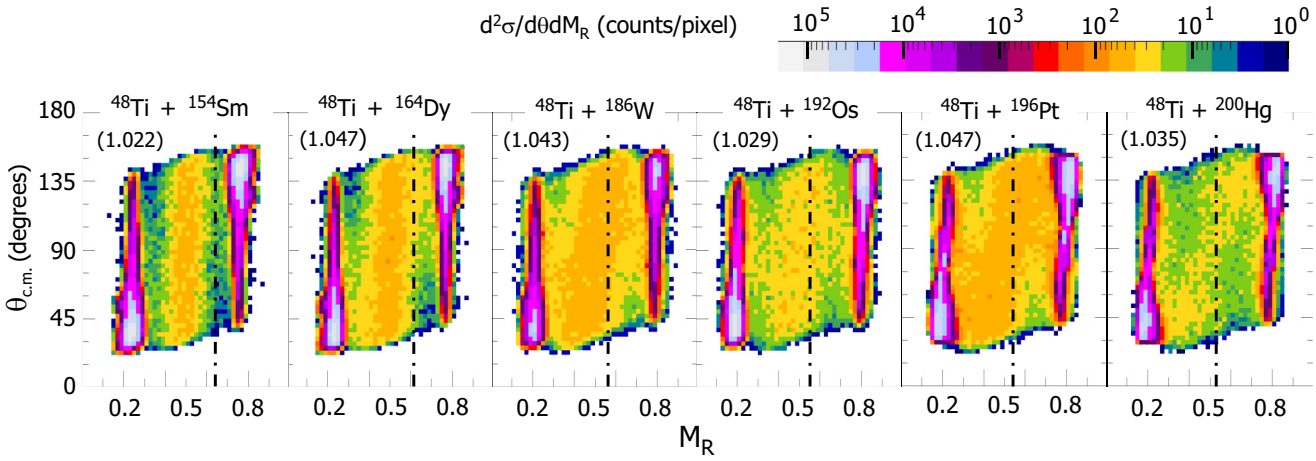

FIG. 1. Mass-angle distributions (MADs) from representative reactions with the lighter targets, and for all targets heavier than ^{178}Hf that were measured in this study. Fission and quasifission lie between the intense quasielastic bands occurring at the mass ratios $M_R \approx 0.2$ and 0.8. The MADs indicate a transition from dominantly fusion-fission for ^{154}Sm to dominantly quasifission for ^{186}W and heavier targets. The MAD for ^{48}Ti + ^{164}Dy suggests the presence of both components with similar yields. The values of E/V_B are given in brackets (see text). The mass-ratio M_R values corresponding to a heavy fragment with $Z = 54$ are indicated by the vertical dot-dashed lines. No clear evidence for enhancements in yield around $Z = 54$ is seen in the MADs.

narrow angle-independent fusion-fission component. Fitting of the mass-ratio spectrum (discussed below) supports this impression and furthermore allows an estimate of the relative probabilities, as described in Sec. III D.

If known shell structure were affecting the observed quasifission, where should evidence be found in the mass spectra? Mass-asymmetric fission of actinide elements is found to be correlated with the heavy-fragment proton number [51].

The lower probability Standard I (StI) mode was found empirically to be centered at $Z = 52.5$, the stronger Standard II (StII) mode at $Z = 55$. In quasifission it would be remarkable if these nearby modes could be separated, so for simplicity in presentation we have chosen to calculate the expected mass ratio where these shell effects may be expected using a weighted average proton number $Z = 54$. Taking the unchanged charge density (UCD) assumption, the mean mass-ratio expected for the heavy fragment is simply 54 divided by the atomic number of the compound nucleus Z_{CN}. The resulting values of M_R for each reaction are shown by the vertical dot-dashed lines in each panel. These move from being well away from mass symmetry ($M_R = 0.5$) for ^{48}Ti + ^{154}Sm to only slightly above symmetry for ^{48}Ti + ^{200}Hg.

The overall trend of the measured MADs moves in the opposite direction to that of the $Z = 54$ line, changing from a narrow distribution peaked at symmetry for ^{48}Ti + ^{154}Sm to a very wide distribution for ^{48}Ti + ^{200}Hg. Furthermore, within each MAD, no localized strong features correlated with $Z = 54$ are apparent, unlike the very obvious peak close to ^{208}Pb seen in quasifission mass distributions and MADs for reactions with heavy actinide nuclei [21,24,33,39,45,71]. Thus a more detailed and quantitative analysis is required, at the lowest measured excitation energies (consistent with sufficient statistics) where shell effects should be largest. This analysis also includes a comparison with measured fission decay mass spectra for isotopes close to the compound nuclei formed in this work.

B. Selecting data for investigation of shell effects

The location of shell structure in M_R should not change with observation angle or with beam energy. Thus to maximize the statistics in the mass-ratio spectra, for each reaction the MADs were integrated over the angular range $40^\circ < \theta_{\text{c.m.}} < 140^\circ$. To focus on the lowest energies, where shell effects should be maximal, the M_R spectra from the two or three lowest E/V_B for each reaction were summed. Having sufficient data at lower energies, it was not necessary to include the higher-energy data shown in Fig. 1 for the ^{186}W and ^{196}Pt reactions. The mean E/V_B and mean excitation energy $\langle E_x \rangle$ values for each reaction were obtained by weighting by the number of fission events collected at each energy.

The resulting "composite" mass-ratio spectra for all reactions are shown in Fig. 2. For clarity of presentation each is normalized to the same yield at mass symmetry. Statistical uncertainties are shown for each data point, which near the peak in yield are typically 2% to 3%. The systematic changes between reactions reflect the changes in the MADs seen in Fig. 1. The transition from dominantly fusion-fission (for ^{154}Sm) to quasifission for the heavier targets is very clear.

Changes in the quasifission mass-width between the heavier targets is also clearly seen. The quasifission mass width in itself is a complex subject. In Ref. [72] the overall mass width for ^{48}Ti reactions was found to depend strongly on E/V_B, the entrance channel fissility, and the magnitude of the quadrupole coupling parameter β_2 (related to the static deformation of these heavy nuclei).

Since the purpose of this work is to investigate evidence for shell structures in the mass spectra, these issues need not be further discussed. This is because evidence of shell effects should be visible as modulations of the yield at M_R values corresponding to relevant shells, relative to a smooth dependence that would be expected in the absence of shell structure.

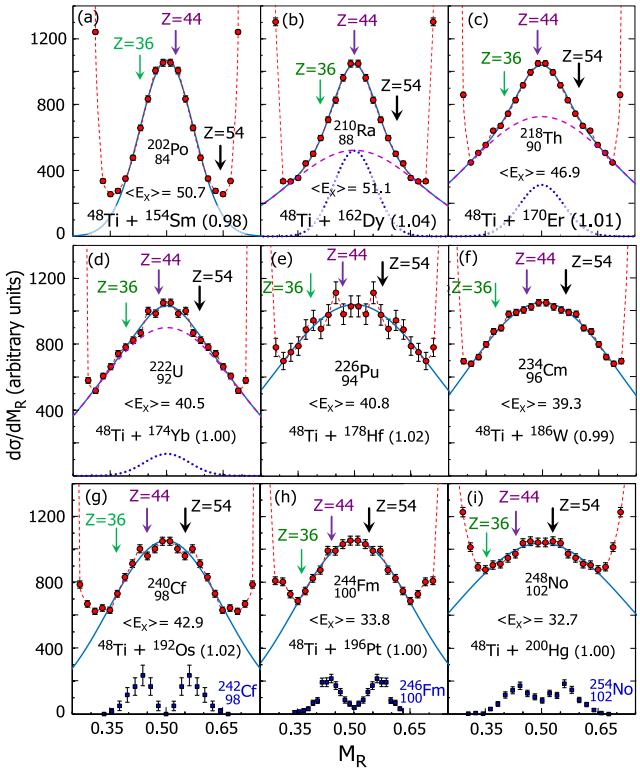

FIG. 2. Mass-ratio M_R spectra for all reactions, with the resulting compound nucleus indicated in each panel. The data are averaged over the lowest two or three beam energies, giving the weighted average E/V_B shown in brackets, and average excitation energies $\langle E_x \rangle$ above the ground-states (in MeV). Gaussian fits are indicated by blue curves (total). Narrow (blue dotted) and wide (red dashed) Gaussians were required [panels (b)–(d)], where fusion-fission and quasifission both contribute significantly. The vertical arrows show the M_R values corresponding to the indicated proton numbers believed to affect fusion-fission (see text). In panels (g)–(i), mass spectra for low-energy fission [68–70] of neighboring nuclides (identified in blue text) are also plotted, showing dominant mass-asymmetric fission. For the quasifission reactions, one or more data points for M_R values slightly above $Z = 54$ lie just above the Gaussian fits.

C. Gaussian fits to the mass spectra

The smooth behavior of yield with M_R has been estimated from a Gaussian fit to the M_R region around symmetry, extending only as far as the M_R values where the yield shows an increase associated with the tail of the intense quasielastic events. Figure 2 shows that a single narrow Gaussian gives a good representation for the $^{48}\mathrm{Ti} + ^{154}\mathrm{Sm}$ reaction, except near $M_R = 0.35$, where a small quasifission contribution was evident in the MAD, as noted above. Equivalent fit quality over a slightly wider mass range was obtained with an almost flat quasifission component underlying a slightly narrower fusion-fission peak. For $^{48}\mathrm{Ti} + ^{178}\mathrm{Hf}$ [Fig. 2(e)] and heavier targets, a single wide Gaussian described the general trend of each distribution very well, with the average χ^2 per degree of freedom being 0.98. This Gaussian is taken as the smooth quasifission behavior.

However, for $^{48}\mathrm{Ti} + ^{162}\mathrm{Dy}$, $^{170}\mathrm{Er}$, and $^{174}\mathrm{Yb}$ only a *two* Gaussian fit could give reasonable χ^2 values, one Gaussian being narrow (representing the fusion-fission component, and indicated by the dotted blue curves) and one wide, representing the quasifission component (indicated by the dashed red curves). The widths and relative probabilities of the fusion-fission components are reasonable, but cannot be relied on in detail, since they are contingent of the distributions of each component actually having a Gaussian form. The presence of two components in these reactions introduces uncertainty in the investigation of possible evidence of shell structure in quasifission for these particular reactions.

For the $^{48}\mathrm{Ti} + ^{178}\mathrm{Hf}$ reaction and heavier, this issue is not significant, since there is no evidence in the data of the narrow fusion-fission component. This is supported by extrapolation of the trends in the fraction of fusion-fission yield as a function of atomic number presented below in Sec. III D. Thus for these reactions deviations from the smooth fits should provide unambiguous evidence of the influence of shells on the quasifission mass distributions. This analysis is presented immediately after Sec. III D below.

D. Evaluation of P_{CN}

The magnitude of any small contribution of fusion-fission to the measured mass spectrum for the heavier systems can be estimated by extrapolating the empirical fusion-fission contributions to higher compound nucleus Z (Z_{CN}). The ratio of the yield of the narrow (fusion-fission) component to the total (fusion-fission plus quasifission) fission yield gives an estimate of the probability P_{CN} that an equilibrated compound nucleus is formed. Note that this is an average over the range of angular momenta populated in capture for each reaction. In determining P_{CN}, the fitted Gaussians shown in Fig. 2 were integrated from mass symmetry up to the entrance-channel mass asymmetry, since there is no experimental evidence in the MADs for significant quasifission yield at larger mass asymmetries.

Extracted values of P_{CN} are shown as a function of Z_{CN} in Fig. 3. They show a rapid fall with increasing Z_{CN}, and have been fit with a Fermi function (dashed line) to aid in extrapolation. For $Z_{CN} = 94$ ($^{48}\mathrm{Ti} + ^{178}\mathrm{Hf}$) this gives an estimate of $P_{CN} = 0.016$, and for $Z_{CN} = 96$ of 0.006. This is very much smaller than the statistical uncertainties of the data points in the M_R spectrum for $Z = 96$, so cannot affect in any significant way the fitting and subsequent interpretation of the quasifission mass distribution for this and heavier systems.

For the purpose of estimating whether fusion-fission contributes significantly to the measured mass distribution for the heavier targets, the quoted empirical values of P_{CN} are appropriate. However, for comparison with model calculations or other measurements, it should be noted that, as empirical values, a number of effects are not accounted for.

The first is that the detector angular coverage from 40° to 140°, although large, is not complete. It may be a reasonable assumption that the angular distributions outside this region are similar for fusion-fission and quasifission in these heavy-ion reactions. However, as noted in Refs. [28,64], this need not be the case.

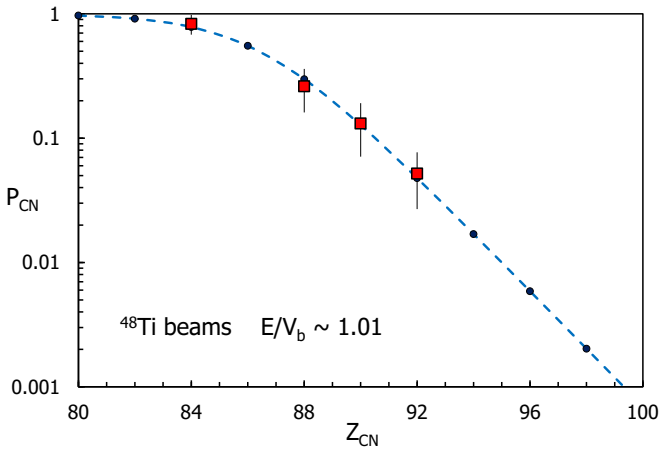

FIG. 3. Ratio of the fusion-fission yield to the total fission yield, obtained from the Gaussian fits integrated over the M_R range between the elastic peaks. This can be identified with the average probability P_{CN} of forming a compound nucleus after capture (see text). Values are plotted as a function of the atomic number of the compound nucleus Z_{CN}. A Fermi function fit is shown by the dashed line (see text). Uncertainties come largely from the unconstrained mass widths of the fit Gaussians.

The second uncertainty is that the evaporation residue cross section (contributing to fusion) is neglected. However, it is expected to be small in these heavy-ion reactions, which form quite neutron-deficient actinide compound nuclei.

The third and probably largest uncertainty arises from the fits themselves. It has been found [73–75] that fusion-fission in heavy-ion reactions may not follow a Gaussian form, but is itself affected by shell structure. Ideally the fusion-fission mass spectrum would be determined experimentally for a reaction with a lighter projectile forming the same compound nucleus under similar conditions. Since this information was not available, initially the fits were completely unconstrained in width and yield. With limited statistics and a small fusion-fission component, this led in some fits to an unexpectedly narrow fusion-fission mass distribution. Thus here a minimum Gaussian sigma in M_R of 0.05 was applied in the fitting to obtain the quoted values of P_{CN}. Conservatively, the uncertainties shown in Fig. 3 correspond to extension down to the best-fit width, and up to a width of 0.07. Furthermore, it is also assumed that the quasifission M_R spectrum follows a Gaussian form both towards mass symmetry, and towards the entrance-channel mass asymmetry.

To address these issues in the fitting procedure, a measurement of the fusion-fission mass spectrum would significantly constrain the fit and allow a much more precise determination of P_{CN}. This is a subject for future work.

E. Extracting evidence for shell structure in the quasifission mass distributions

All quasifission M_R spectra in this work are found to be peaked at mass symmetry ($M_R = 0.5$), unlike low-energy fission of actinide nuclei, which typically show peak yields at M_R around 0.57. This suggests that the effect of shells is not the same in quasifission.

The deviations of the experimental M_R spectra from the smooth fits (full blue curves in Fig. 2) are clearly small, with points typically deviating from the fits within their statistical uncertainties. This is quantified by the χ^2 per degree of freedom of the fits, which averages 0.98 for the single-Gaussian quasifission-only fits. A few points in each spectrum lie away from the fit, but this is expected when fitting data with statistical scatter.

1. Expectations for shell structure systematics

A particular shell gap will appear at different M_R depending on the charge and mass of the compound nucleus. Thus if shell structure were present in the M_R distributions, it should follow a systematic pattern as the compound nucleus charge and mass change. Which shells are expected to be important? As already discussed, $Z = 54$ (black arrows in Fig. 2) represents the average of the Standard I and Standard II mass-asymmetric fission modes seen in low-energy fission of most actinide nuclides. For completeness, other potential shell gaps should be considered.

Different proton shell gaps are believed to play a role in fission of lighter nuclei, around and lighter than ^{208}Pb [75–77]. The position in M_R of proposed important proton shells are indicated by the green ($Z = 36$) and purple ($Z = 44$) arrows in Fig. 2. Because of the different dynamics of quasifission compared with fusion-fission, as discussed above, it could be that they play a more significant role in quasifission. Although $Z = 44$ is close to the peak (fusion-fission) yield in the three lightest systems, there is no evidence of significant deviations from the smooth fits for the heavier systems that are systematically correlated with these proton numbers.

Having considered shell gaps in the light quasifission fragments, believed to affect fusion-fission mass distributions of lighter nuclei, we return now to the shell gaps in the heavy quasifission fragments understood to play the dominant role. First it should be noted that the heavy nuclei created following capture in these reactions are significantly more neutron-deficient than those generally associated with the Standard I and Standard II modes.

To investigate experimentally whether this is important, measured mass spectra converted to M_R (black squares) for low-energy fission of the heaviest elements studied, neutron-deficient ^{242}Cf [68], ^{246}Fm [69], and ^{254}No [70] are shown in Figs. 2(g) to 2(i). They show similar mass-asymmetric fission to other actinides. The highest yield in each experimental spectrum can be converted to the proton number of the heavy fragment using the UCD assumption, giving $Z = 55$, 56, and 57 respectively, with an average of $Z = 56$. Thus if quasifission follows the same shell valley(s) in the PES, the shell structure in quasifission might be expected at M_R values slightly above the M_R values predicted for $Z = 54$.

The semi-empirical GEF model [78] can be used to predict the compound nucleus fission-mass distributions for the actual compound nuclei formed in this study, for which (to our knowledge) no low-energy fission data exist. For the slightly more neutron-deficient isotopes ^{240}Cf, ^{244}Fm, and ^{248}No that

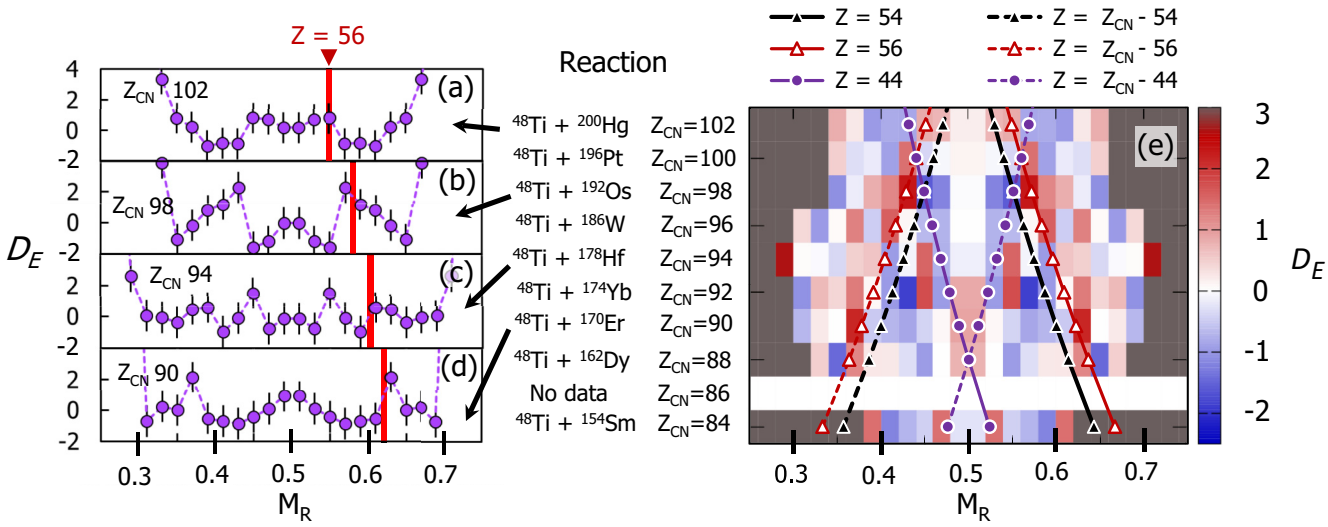

FIG. 4. The deviation from a Gaussian fit to the mass-ratio M_R spectrum divided by the statistical uncertainty of each experimental data point is defined as D_E (see text). Panels (a) to (d) show values of D_E as a function of M_R for four of the reactions. The red bars correspond to the location of a fragment with $Z = 56$ for each reaction. Panel (e) shows D_E for all reactions studied, in a two-dimensional representation, as a function of M_R and the atomic number of the composite nuclei Z_{CN} populated in the reactions indicated. The values of D_E are represented by the color scale on the right, with values of three and over in dark brown. The overlaid circles and triangles show the positions of the proton numbers understood to influence the low-energy fission-mass spectra for actinide nuclides (see text). The red triangles at $Z = 56$ are correlated with a slight systematic excess of yield in most reactions, with the largest excesses shown in panels (b) and (d).

are formed in the ^{48}Ti reactions, GEF model calculations at low E_x predict dominant mass-asymmetric fission. This means that the mass-asymmetric fission barriers are calculated to be the lowest. For ^{222}U, ^{226}Pu, and ^{234}Cm, the GEF calculations predict fission peaked at mass symmetry, meaning that that the calculated mass-symmetric barriers are lowest. However, the height of the fission barrier itself is not expected to play a direct role in quasifission mass distributions. The mass-asymmetric valleys outside the barriers will still be present even if the fission barriers leading to them are not the lowest, and they would be expected to have a similar effect on the quasifission dynamics for the reactions forming these nuclides ^{222}U, ^{226}Pu, and ^{234}Cm also.

2. *Systematic search for experimental shell effects*

Close inspection of the M_R spectra in Fig. 2 shows that typically one or two points in each spectrum at M_R values slightly higher than the positions of the arrows indicating $Z = 54$ lie consistently above the smooth fits. This deviation corresponds typically to slightly more than one standard deviation, or typically around 3%. In any one spectrum, this could simply be by chance. However, consistent deviations, not at a fixed M_R but at a variable M_R that is correlated with expectations for shell effects, would suggest that shells in the heavy fragment might be having a small influence on quasifission mass distributions.

To highlight and quantify systematically these small effects, the deviations (residuals) from the smooth fits have been evaluated by subtracting the fit value from the experimental value. A low-statistics spectrum would be expected to show larger deviations due to random fluctuations than a high-statistics spectrum. The significance of a fluctuation is quantified by the size of the deviation relative to the uncertainty of the experimental value. Dividing the deviations by the experimental uncertainty in $d\sigma/dM_R$ yields the normalized experimental deviation D_E, which quantifies the statistical significance of the deviation. D_E has been evaluated for each data point in the M_R spectrum, for each reaction.

Examples of D_E spectra as a function of M_R for four reactions (each separated in Z_{CN} by four) are shown in Figs. 4(a)–4(d). The uncertainty on each point is ± 1 by construction, so all points from all spectra have the same statistical significance. Fluctuations from zero are seen for all spectra, as expected. The question is, are they correlated with particular shells?

The M_R values associated with a particular proton shell gap (Z_{shell}) can be calculated assuming that the A/Z ratio of the fragments is the same as that of the compound nucleus (unchanged charge-density assumption). Thus, $M_R = Z_{\text{shell}}/Z_{CN}$. As an example, the positions in M_R for $Z = 56$ (the experimental position of the peak yield for low-energy fission of the three heaviest systems) are shown by the vertical red bars. Two of the spectra show a significant positive deviation of slightly over two standard deviations close to the red bars, while two do not. Thus no conclusive evidence is seen here for a consistent excess in yield around $Z = 56$. With more experimental D_E spectra, and potentially more shells, the search for evidence could become quite complex.

To attempt to simplify visual assessment of possible correlations, a two-dimensional representation of the systematic behavior of D_E is shown in Fig. 4(e). Here the values of D_E are indicated by the color scale as a function of M_R on the x axis, and the Z of the compound nucleus (Z_{CN}) on the y axis. An excess in experimental yield over the fit that corresponds to

two standard deviations (2σ) has the value $+2$ (red shading), while a 2σ deficit in yield takes the value -2 (blue shading), as indicated on the color key on the far right.

Possible correlations with other proton shells understood to affect fission are discussed first. M_R values for $Z = 54$ are indicated by the black triangles joined by the full black line (heavy fragment) or dashed line (correlated light fragment). The $Z = 54$ line is actually systematically correlated with a deficit of yield with respect to the fits. Also shown is the locus expected for $Z = 44$ (purple circles). This is correlated with slightly enhanced yield near mass symmetry for $Z_{CN} < 92$, associated with the fusion-fission component in the mass distributions for these reactions. This correlation with $Z = 44$ is consistent with the experimental fusion-fission mass distributions presented in Ref. [75]. However, $Z = 44$ is not correlated with consistent positive deviations from the fits for the heavier systems.

The $Z = 56$ locus (white triangles outlined in red) is generally associated with excess yield (pink or red shading), only the data for $Z_{CN} = 54$ having a deficit in yield at the $Z = 56$ line. The excess is, however, hardly more than one standard deviation on average. The rapid change from excess ($Z = 56$) to deficit ($Z = 54$) seen in the graph might throw doubt on whether the excess could be due to a physical correlation with shells. However, a smooth fit to data including a modulation will give a maximum at the peak position, and minima either side, over the region of the modulation. This behavior is illustrated in Fig. 5(c) in a fit to a calculated mass spectrum. Thus the observed experimental behavior may be consistent with a shell effect. However, it is clear that any effect of shells in these quasifission reactions is at the limits of visibility.

Even with 2%–3% statistical uncertainties at each M_R value in the experimental quasifission M_R spectra, and systematic measurements for nine different compound nuclei from $Z_{CN} = 84$ to 102, it has proven difficult to find conclusive evidence that shell effects play a role in determining the quasifission mass division. Unless the effect of shells on quasifission dynamics is very different from their effect on fission, it must be concluded that the effect of shells on these quasifission mass spectra appears to be very weak.

3. *Effect of excitation energy*

The location and effect of shells is well established in low-energy fission of these actinide nuclides. The question is why their effect on mass distributions appears to be small when these nuclei are formed in quasifission reactions. The answer may lie in the excitation energies, which are 33 MeV or more in the quasifission reactions studied. Excitation energy is expected to attenuate shell effects because excitations across a shell gap in the single-particle levels reduces the effect of the gap on the total energy of the system. In this picture, at sufficiently high excitation energy, shell effects will be completely "washed out," having no effect on the potential-energy surface.

To determine quantitatively the influence of excitation energy on shells, calculations using the GEF fission code [78] are informative. GEF incorporates the consensus understanding of the quantitative washing out of shell effects with excitation energy, and calculates the effect on fission-mass distributions. As noted above, it is the shell effects at the fission barrier configurations that are relevant in GEF, which does not consider their effects outside the barrier. However, the washing out of shell effects with excitation energy is expected to be a general phenomenon occurring at all deformations. Thus the results should be indicative of the effects of excitation energy also at configurations outside the barrier, relevant to quasifission.

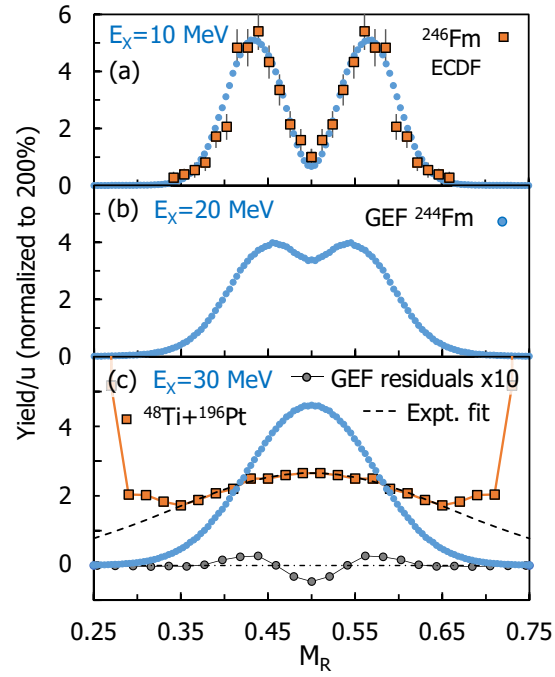

FIG. 5. Fission mass-ratio distributions for first-chance fission of ^{244}Fm, calculated using the GEF code (2021), are shown by blue points for excitation energies E_x above the ground-state of 10, 20, and 30 MeV. At (a) $E_x = 10$ MeV, the experimental (mass-asymmetric) low-energy fission [69] of ^{246}Fm following electron capture—ECDF—(orange points) is in good agreement. Panel (b) shows that, at 20 MeV, the mass-symmetric mode is dominant. At 30 MeV, the mass-symmetric liquid drop mode is calculated to comprise over 98% of the yield: shell effects have essentially disappeared. Only by fitting a Gaussian to the calculation are the shell effects revealed in the residuals, shown by the joined gray circles (see text).

The quasifission timescale for these reactions is expected to be $\approx 10^{-20}$ s [20,67]. This is less than the times expected for fusion-fission [79–82] from the ground-state, particularly at the excitation energies populated here for the heavier systems. Thus the excitation energy relevant to quasifission should be that of first-chance fission alone, which can be specified for the GEF calculations.

For comparison with the experimental results, fission mass-ratio distributions at scission have been generated from GEF-2021 [83]. Calculated first-chance fission-mass distributions for fission of ^{244}Fm (formed experimentally in the ^{48}Ti + ^{196}Pt reaction) at excitation energies above the ground-state of 10, 20, and 30 MeV are shown in Fig. 5.

At the lowest E_x of 10 MeV, shown in Fig. 5(a), the calculated first-chance mass distribution is dominated by the

asymmetric Standard I and Standard II modes (originating from shell effects), which empirically are found to be centered at $Z = 52.5$ and 55. The symmetric (liquid drop) mode comprises only ≈6% of the fission yield. The experimental [69] electron-capture delayed fission (ECDF) mass-ratio distribution for the neighboring nucleus ^{246}Fm is shown by orange squares, agreeing well with the GEF calculations.

Already at $E_x = 20$ MeV, shown in Fig. 5(b), the mass-symmetric (liquid drop) mode is calculated to be dominant, comprising 66% of the total fission yield. Nevertheless the presence of the 34% contribution from the asymmetric modes is still clearly visible.

At $E_x = 30$ MeV [Fig. 5(c)], the calculated contribution from the mass-asymmetric modes is less than 2%, with the liquid drop mass-symmetric mode completely dominant. Thus at the mean excitation energy of the ^{48}Ti + ^{196}Pt measurements (36 MeV) GEF predicts that mass-asymmetric fission originating from shell effects is almost completely suppressed. Note also that the excitation energy above the PES *outside* the fission barrier (relevant for quasifission) will by definition be higher than that *at* the fission barrier, which is relevant to the GEF calculations of fusion-fission. The reduction with excitation energy of the effects of shell gaps may well explain the minimal evidence for shell structure seen in the experimental quasifission mass distributions.

The GEF calculation at 30 MeV gives an opportunity to test the technique used with the experimental quasifission mass spectra to reveal evidence of shell structure. The residuals from a single Gaussian fit are shown in Fig. 5(c), scaled up by a factor of two, and summed into five mass unit bins, similar to the experimental ^{48}Ti + ^{196}Pt data. This gives an effective increase in visibility of a factor of 10. The peak in the residuals corresponds closely to the peak in yield at $E_x =$ 10 MeV. As expected, the peak has negative residuals on either side, resulting in a narrower feature in the residuals than in the actual mass spectrum, with only two mass bins significantly above zero (dot-dashed line). Thus without knowledge of the position of shell structure, a weak modulation is successfully revealed by this technique. It does rely on the smooth behavior following closely a Gaussian form, which is clearly the case in these calculations.

The suggestion that excitation energy may be the reason for the small influence of shell effects seen in quasifission (corresponding to deformations outside the fission barrier) could be tested quantitatively with a Langevin calculation of the quasifission mass distributions resulting from motion over a PES where the effect of shells has been attenuated in the same way as in GEF.

Before concluding this comparison with GEF calculations, it should be noted that the width of the calculated mass-symmetric (liquid drop) fission mode is much smaller than that of the measured quasifission distribution in the heavy-ion reaction (shown in Fig. 5(c) by the orange squares, and its Gaussian fit by the dashed curve). Together with the experimental mass-angle correlation, it is clear that the quasifission occurs well before equilibration of the degrees of freedom that determine the mass distribution.

IV. SUMMARY AND CONCLUSIONS

Systematic measurements have been made of mass-angle distributions at beam energies near the respective capture barrier energies (where quasifission is most prominent) for fission following collisions of ^{48}Ti projectiles with even-even nuclides from ^{154}Sm to ^{200}Hg. Excitation energies above the respective ground-states ranged from 51 to 33 MeV, respectively.

With increasing target (or equivalently compound nucleus) atomic number, a rapid transition occurs from dominant fusion-fission to dominantly quasifission (with angle-integrated yield peaked at mass-symmetry, corresponding to mass-angle distributions of type 2 in Ref. [20]). The heaviest reactions form ^{240}Cf, ^{244}Fm, and ^{248}No, where experimental-low energy fission mass distributions of neighboring isotopes are mass asymmetric, correlated with proton number $Z = 56$ in the heavy fragment.

No significant (>3%) systematic features are seen in any single quasifission mass spectrum correlated with known proton shells, including proton shells at $Z \approx 36$ and 44, understood to give rise to mass-asymmetric fission in pre-actinide nuclei.

A novel approach to combine all the experimental results suggests a small (≈3%) systematic excess of yield correlated with $Z = 56$, however this is at the limit of sensitivity of the experiment. It is concluded that evidence for the effect of shells on these quasifission mass distributions is weak.

It is suggested that this may be because of significant attenuation of shell effects resulting from the excitation energy introduced in the heavy-ion reactions, even for measurements at the capture barrier energies. These excitation energies are typical of the reactions used to synthesize superheavy elements in fusion reactions with actinide nuclides. The results suggest that attenuation of shell effects should be significant in those reactions also.

ACKNOWLEDGMENTS

The authors acknowledge the Australian Research Council for support through Discovery Grants No. DP170102318, DP190101442, DP190100256, and DP200100601. Financial support for accelerator operations was provided by the National Collaborative Research Infrastructure Strategy (NCRIS) through the Heavy Ion Accelerators (HIA) project.

[1] P. Möller, EPJ Web Conf. **131**, 03002 (2016).
[2] S. Hofmann and G. Münzenberg, Rev. Mod. Phys. **72**, 733 (2000).
[3] Yu. Ts. Oganessian, V. K. Utyonkov, Y. V. Lobanov, F. S. Abdullin, A. N. Polyakov, I. V. Shirokovsky, Y. S. Tsyganov, G. G. Gulbekian, S. L. Bogomolov, B. N. Gikal, A. N. Mezentsev, S. Iliev, V. G. Subbotin, A. M. Sukhov, A. A. Voinov, G. V. Buklanov, K. Subotic, V. I. Zagrebaev, M. G. Itkis, J. B. Patin *et al.*, Phys. Rev. C **70**, 064609 (2004).

[4] K. Morita, K. Morimoto, D. Kaji, T. Akiyama, S. ichi Goto, H. Haba, E. Ideguchi, R. Kanungo, K. Katori, H. Koura, H. Kudo, T. Ohnishi, A. Ozawa, T. Suda, K. Sueki, H. Xu, T. Yamaguchi, A. Yoneda, A. Yoshida, and Y. Zhao, J. Phys. Soc. Jpn. **73**, 2593 (2004).

[5] Yu. Ts. Oganessian, V. K. Utyonkov, Y. V. Lobanov, F. S. Abdullin, A. N. Polyakov, R. N. Sagaidak, I. V. Shirokovsky, Y. S. Tsyganov, A. Voinov, G. Gulbekian, S. Bogomolov, B. Gikal, A. Mezentsev, S. Iliev, V. Subbotin, A. Sukhov, K. Subotic, V. Zagrebaev, G. Vostokin, M. Itkis *et al.*, Phys. Rev. C **74**, 044602 (2006).

[6] Yu. Ts. Oganessian, F. S. Abdullin, P. D. Bailey, D. E. Benker, M. E. Bennett, S. N. Dmitriev, J. G. Ezold, J. H. Hamilton, R. A. Henderson, M. G. Itkis, Y. V. Lobanov, A. N. Mezentsev, K. J. Moody, S. L. Nelson, A. N. Polyakov, C. E. Porter, A. V. Ramayya, F. D. Riley, J. B. Roberto, M. A. Ryabinin *et al.*, Phys. Rev. Lett. **104**, 142502 (2010).

[7] Y. T. Oganessian, F. S. Abdullin, C. Alexander, J. Binder, R. A. Boll, S. N. Dmitriev, J. Ezold, K. Felker, J. M. Gostic, R. K. Grzywacz, J. H. Hamilton, R. A. Henderson, M. G. Itkis, K. Miernik, D. Miller, K. J. Moody, A. N. Polyakov, A. V. Ramayya, J. B. Roberto, M. A. Ryabinin *et al.*, Phys. Rev. Lett. **109**, 162501 (2012).

[8] B. B. Back, Phys. Rev. C **31**, 2104 (1985).

[9] J. Tõke, B. Bock, G. X. Dai, A. Gobbi, S. Gralla, K. D. Hildenbrand, J. Kuzminski, W. F. J. Müller, A. Olmi, and H. Stelzer, Nucl. Phys. A **440**, 327 (1985).

[10] E. Vardaci, M. G. Itkis, I. M. Itkis, G. Knyazheva, and E. M. Kozulin, J. Phys. G **46**, 103002 (2019).

[11] D. J. Hinde, M. Dasgupta, and E. C. Simpson, Prog. Part. Nucl. Phys. **118**, 103856 (2021).

[12] J. Maruhn, W. Greiner, and W. Scheid, *Heavy Ion Collisions*, edited by R. Bock (North-Holland, Amsterdam, 1980), Vol. 2, p. 398.

[13] D. J. Hinde and M. Dasgupta, Phys. Lett. B **622**, 23 (2005).

[14] C. Simenel, D. J. Hinde, R. du Rietz, M. Dasgupta, M. Evers, C. J. Lin, D. H. Luong, and A. Wakhle, Phys. Lett. B **710**, 607 (2012).

[15] G. Mohanto, D. J. Hinde, K. Banerjee, M. Dasgupta, D. Y. Jeung, C. Simenel, E. C. Simpson, A. Wakhle, E. Williams, I. P. Carter, K. J. Cook, D. H. Luong, C. S. Palshetkar, and D. C. Rafferty, Phys. Rev. C **97**, 054603 (2018).

[16] J. Khuyagbaatar, H. M. David, D. J. Hinde, I. P. Carter, K. J. Cook, M. Dasgupta, Ch. E.. Düllmann, D. Y. Jeung, B. Kindler, B. Lommel, D. H. Luong, E. Prasad, D. C. Rafferty, C. Sengupta, C. Simenel, E. C. Simpson, J. F. Smith, K. Vo-Phuoc, J. Walshe, A. Wakhle *et al.*, Phys. Rev. C **97**, 064618 (2018).

[17] K. Banerjee, D. J. Hinde, M. Dasgupta, E. C. Simpson, D. Y. Jeung, C. Simenel, B. M. A. Swinton-Bland, E. Williams, I. P. Carter, K. J. Cook, H. M. David, Ch. E.. Düllmann, J. Khuyagbaatar, B. Kindler, B. Lommel, E. Prasad, C. Sengupta, J. F. Smith, K. Vo-Phuoc, J. Walshe *et al.*, Phys. Rev. Lett. **122**, 232503 (2019).

[18] E. M. Kozulin, G. N. Knyazheva, K. V. Novikov, I. M. Itkis, M. G. Itkis, S. N. Dmitriev, Y. T. Oganessian, A. A. Bogachev, N. I. Kozulina, I. Harca, W. H. Trzaska, and T. K. Ghosh, Phys. Rev. C **94**, 054613 (2016).

[19] E. M. Kozulin, G. N. Knyazheva, T. K. Ghosh, A. Sen, I. M. Itkis, M. G. Itkis, K. V. Novikov, I. N. Diatlov, I. V. Pchelintsev, C. Bhattacharya, S. Bhattacharya, K. Banerjee, E. O. Saveleva, and I. V. Vorobiev, Phys. Rev. C **99**, 014616 (2019).

[20] R. du Rietz, E. Williams, D. J. Hinde, M. Dasgupta, M. Evers, C. J. Lin, D. H. Luong, C. Simenel, and A. Wakhle, Phys. Rev. C **88**, 054618 (2013).

[21] H. Albers, J. Khuyagbaatar, D. Hinde, I. Carter, K. Cook, M. Dasgupta, Ch. E.. Düllmann, K. Eberhardt, D. Jeung, S. Kalkal, B. Kindler, N. Lobanov, B. Lommel, C. Mokry, E. Prasad, D. Rafferty, J. Runke, K. Sekizawa, C. Sengupta, C. Simenel *et al.*, Phys. Lett. B **808**, 135626 (2020).

[22] R. Kalpakchieva, Y. Oganessian, Y. Penionzhkevich, and H. Sodan, Z. Phys. A: At. Nucl. (1975) **283**, 253 (1977).

[23] P. Gippner, K. D. Schilling, W. Seidel, F. Stary, E. Will, H. Sodan, S. M. Lukyanov, V. S. Salamatin, Y. E. Penionzhkevich, G. G. Chubarian, and R. Schmidt, Z. Phys. A **325**, 335 (1986).

[24] M. Itkis, J. Äystö, S. Beghini, A. Bogachev, L. Corradi, O. Dorvaux, A. Gadea, G. Giardina, F. Hanappe, I. Itkis, M. Jandel, J. Kliman, S. Khlebnikov, G. Kniajeva, N. Kondratiev, E. Kozulin, L. Krupa, A. Latina, T. Materna, G. Montagnoli *et al.*, Nucl. Phys. A **734**, 136 (2004).

[25] M. Itkis, A. Bogachev, I. Itkis, J. Kliman, G. Knyazheva, N. Kondratiev, E. Kozulin, L. Krupa, Y. Oganessian, I. Pokrovsky, E. Prokhorova, and A. Rusanov, Nucl. Phys. A **787**, 150 (2007).

[26] E. M. Kozulin, G. N. Knyazheva, I. M. Itkis, M. G. Itkis, A. A. Bogachev, L. Krupa, T. A. Loktev, S. V. Smirnov, V. I. Zagrebaev, J. Äystö, W. H. Trzaska, V. A. Rubchenya, E. Vardaci, A. M. Stefanini, M. Cinausero, L. Corradi, E. Fioretto, P. Mason, G. F. Prete, R. Silvestri *et al.*, Phys. Lett. B **686**, 227 (2010).

[27] M. G. Itkis, Y. T. Oganessian, and V. I. Zagrebaev, Phys. Rev. C **65**, 044602 (2002).

[28] E. Prasad, A. Wakhle, D. J. Hinde, E. Williams, M. Dasgupta, M. Evers, D. H. Luong, G. Mohanto, C. Simenel, and K. Vo-Phuoc, Phys. Rev. C **93**, 024607 (2016).

[29] C. Simenel, P. McGlynn, A. S. Umar, and K. Godbey, Phys. Lett. B **822**, 136648 (2021).

[30] A. N. Andreyev, K. Nishio, and K.-H. Schmidt, Rep. Prog. Phys. **81**, 016301 (2018).

[31] Y. Aritomo, Nucl. Phys. A **780**, 222 (2006).

[32] Y. Aritomo, Phys. Rev. C **80**, 064604 (2009).

[33] G. N. Knyazheva, I. M. Itkis, and E. M. Kozulin, J. Phys.: Conf. Ser. **515**, 012009 (2014).

[34] H. J. Rose and G. A. Jones, Nature (London) **307**, 245 (1984).

[35] D. J. Hinde, R. du Rietz, M. Dasgupta, R. G. Thomas, and L. R. Gasques, Phys. Rev. Lett. **101**, 092701 (2008).

[36] K. Nishio, H. Ikezoe, S. Mitsuoka, I. Nishinaka, Y. Nagame, Y. Watanabe, T. Ohtsuki, K. Hirose, and S. Hofmann, Phys. Rev. C **77**, 064607 (2008).

[37] K. Nishio, S. Mitsuoka, I. Nishinaka, H. Makii, Y. Wakabayashi, H. Ikezoe, K. Hirose, T. Ohtsuki, Y. Aritomo, and S. Hofmann, Phys. Rev. C **86**, 034608 (2012).

[38] I. M. Itkis, E. M. Kozulin, M. G. Itkis, G. N. Knyazheva, A. A. Bogachev, E. V. Chernysheva, L. Krupa, Y. T. Oganessian, V. I. Zagrebaev, A. Y. Rusanov, F. Gönnenwein, O. Dorvaux, L. Stuttgé, F. Hanappe, E. Vardaci, and E. de Goés Brennand, Phys. Rev. C **83**, 064613 (2011).

[39] M. Morjean, D. J. Hinde, C. Simenel, D. Y. Jeung, M. Airiau, K. J. Cook, M. Dasgupta, A. Drouart, D. Jacquet, S. Kalkal, C. S. Palshetkar, E. Prasad, D. Rafferty, E. C. Simpson, L. Tassan-Got, K. Vo-Phuoc, and E. Williams, Phys. Rev. Lett. **119**, 222502 (2017).

[40] D. J. Hinde, D. Y. Jeung, E. Prasad, A. Wakhle, M. Dasgupta, M. Evers, D. H. Luong, R. du Rietz, C. Simenel, E. C. Simpson, and E. Williams, Phys. Rev. C **97**, 024616 (2018).

[41] Y. Abe, C. Gregoire, and H. Delagrange, J. Phys. Colloq. **47**, 329 (1986).

[42] T. Wada, N. Carjan, and Y. Abe, Nucl. Phys. A **538**, 283 (1992).

[43] P. Fröbrich and I. I. Gontchar, Phys. Rep. **292**, 131 (1998).

[44] V. I. Zagrebaev and W. Greiner, J. Phys. G **31**, 825 (2005).

[45] A. Wakhle, C. Simenel, D. J. Hinde, M. Dasgupta, M. Evers, D. H. Luong, R. du Rietz, and E. Williams, Phys. Rev. Lett. **113**, 182502 (2014).

[46] K. Godbey, A. S. Umar, and C. Simenel, Phys. Rev. C **100**, 024610 (2019).

[47] J. V. Kratz, A. E. Norris, and G. T. Seaborg, Phys. Rev. Lett. **33**, 502 (1974).

[48] G. Guarino, A. Gobbi, K. Hildenbrand, W. Möller, A. Olmi, H. Sann, S. Bjørnholm, and G. Rudolf, Nucl. Phys. A **424**, 157 (1984).

[49] E. M. Kozulin, G. N. Knyazheva, I. M. Itkis, M. G. Itkis, A. A. Bogachev, E. V. Chernysheva, L. Krupa, F. Hanappe, O. Dorvaux, L. Stuttgé, W. H. Trzaska, C. Schmitt, and G. Chubarian, Phys. Rev. C **90**, 054608 (2014).

[50] K.-H. Schmidt, S. Steinhauser, C. Bockstiegel, A. Grewe, A. Heinz, A. Junghans, J. Benlliure, H. Clerc, M. de Jong, J. Muller, M. Pfutzner, and B. Voss, Nucl. Phys. A **665**, 221 (2000).

[51] C. Böckstiegel, S. Steinhauser, K.-H. Schmidt, H.-G. Clerc, A. Grewe, A. Heinz, M. de Jong, A. Junghans, J. Muller, and B. Voss, Nucl. Phys. A **802**, 12 (2008).

[52] C. J. Lin, R. du Rietz, D. J. Hinde, M. Dasgupta, R. G. Thomas, M. L. Brown, M. Evers, L. R. Gasques, and M. D. Rodriguez, Phys. Rev. C **85**, 014611 (2012).

[53] W. J. Świątecki, K. Siwek-Wilczyńska, and J. Wilczyński, Phys. Rev. C **71**, 014602 (2005).

[54] J. R. Leigh, M. Dasgupta, D. J. Hinde, J. C. Mein, C. R. Morton, R. C. Lemmon, J. P. Lestone, J. O. Newton, H. Timmers, J. X. Wei, and N. Rowley, Phys. Rev. C **52**, 3151 (1995).

[55] M. Dasgupta, D. J. Hinde, N. Rowley, and A. M. Stefanini, Annu. Rev. Nucl. Part. Sci. **48**, 401 (1998).

[56] D. J. Hinde, M. Dasgupta, J. R. Leigh, J. P. Lestone, J. C. Mein, C. R. Morton, J. O. Newton, and H. Timmers, Phys. Rev. Lett. **74**, 1295 (1995).

[57] J. C. Mein, D. J. Hinde, M. Dasgupta, J. R. Leigh, J. O. Newton, and H. Timmers, Phys. Rev. C **55**, R995 (1997).

[58] D. J. Hinde, A. C. Berriman, R. D. Butt, M. Dasgupta, C. R. Morton, A. Mukherjee, and J. O. Newton, Eur. Phys. J. A **13**, 149 (2002).

[59] D. J. Hinde, M. Dasgupta, J. R. Leigh, J. C. Mein, C. R. Morton, J. O. Newton, and H. Timmers, Phys. Rev. C **53**, 1290 (1996).

[60] R. Rafiei, R. G. Thomas, D. J. Hinde, M. Dasgupta, C. R. Morton, L. R. Gasques, M. L. Brown, and M. D. Rodriguez, Phys. Rev. C **77**, 024606 (2008).

[61] R. G. Thomas, D. J. Hinde, D. Duniec, F. Zenke, M. Dasgupta, M. L. Brown, M. Evers, L. R. Gasques, M. D. Rodriguez, and A. Diaz-Torres, Phys. Rev. C **77**, 034610 (2008).

[62] G. N. Knyazheva, E. M. Kozulin, R. N. Sagaidak, A. Y. Chizhov, M. G. Itkis, N. A. Kondratiev, V. M. Voskressensky, A. M. Stefanini, B. R. Behera, L. Corradi, E. Fioretto, A. Gadea, A. Latina, S. Szilner, M. Trotta, S. Beghini, G. Montagnoli, F. Scarlassara, F. Haas, N. Rowley *et al.*, Phys. Rev. C **75**, 064602 (2007).

[63] W. Q. Shen, J. Albinski, A. Gobbi, S. Gralla, K. D. Hildenbrand, N. Herrmann, J. Kuzminski, W. F. J. Müller, H. Stelzer, J. Tōke, B. B. Back, S. Bjørnholm, and S. P. Sørensen, Phys. Rev. C **36**, 115 (1987).

[64] D. Y. Jeung, D. J. Hinde, E. Williams, M. Dasgupta, E. C. Simpson, R. du Rietz, D. H. Luong, R. Rafiei, M. Evers, I. P. Carter, K. Ramachandran, C. Palshetkar, D. C. Rafferty, C. Simenel, and A. Wakhle, Phys. Rev. C **103**, 034603 (2021).

[65] B. B. Back, R. R. Betts, K. Cassidy, B. G. Glagola, J. E. Gindler, L. E. Glendenin, and B. D. Wilkins, Phys. Rev. Lett. **50**, 818 (1983).

[66] T. Tanaka, D. J. Hinde, M. Dasgupta, E. Williams, K. Vo-Phuoc, C. Simenel, E. C. Simpson, D. Y. Jeung, I. P. Carter, K. J. Cook, N. R. Lobanov, D. H. Luong, C. Palshetkar, D. C. Rafferty, and K. Ramachandran, Phys. Rev. Lett. **127**, 222501 (2021).

[67] R. du Rietz, D. J. Hinde, M. Dasgupta, R. G. Thomas, L. R. Gasques, M. Evers, N. Lobanov, and A. Wakhle, Phys. Rev. Lett. **106**, 052701 (2011).

[68] D. A. Shaughnessy, J. L. Adams, K. E. Gregorich, M. R. Lane, C. A. Laue, D. M. Lee, C. A. McGrath, J. B. Patin, D. A. Strellis, E. R. Sylwester, P. A. Wilk, and D. C. Hoffman, Phys. Rev. C **61**, 044609 (2000).

[69] D. Hoffman, D. Lee, A. Ghiorso, M. Nurmia, and K. Aleklett, Phys. Rev. C **22**, 1581 (1980).

[70] J. Wild, E. Hulet, R. Lougheed, K. Moody, B. Bandong, R. Dougan, and A. Veeck, J. Alloys Compd. **213-214**, 86 (1994).

[71] K. Banerjee, D. J. Hinde, M. Dasgupta, J. Sadhukhan, E. C. Simpson, D. Y. Jeung, C. Simenel, B. M. A. Swinton-Bland, E. Williams, L. T. Bezzina, I. P. Carter, K. J. Cook, H. M. Albers, Ch. E.. Düllmann, J. Khuyagbaatar, B. Kindler, B. Lommel, C. Mokry, E. Prasad, J. Runke *et al.*, Phys. Lett. B **820**, 136601 (2021).

[72] C. J. Lin, H. Q. Zhang, H. M. Jia, F. Yang, Z. H. Liu, X. X. Xu, L. Yang, P. F. Bao, L. J. Sun, K. Nishio, H. Ikezoe, S. Mitsuoka, and K. Satou, J. Phys.: Conf. Ser. **420**, 012126 (2013).

[73] E. Prasad, D. J. Hinde, K. Ramachandran, E. Williams, M. Dasgupta, I. P. Carter, K. J. Cook, D. Y. Jeung, D. H. Luong, S. McNeil, C. S. Palshetkar, D. C. Rafferty, C. Simenel, A. Wakhle, J. Khuyagbaatar, Ch. E.. Düllmann, B. Lommel, and B. Kindler, Phys. Rev. C **91**, 064605 (2015).

[74] K. Nishio, A. Andreyev, R. Chapman, X. Derkx, Ch. E.. Düllmann, L. Ghys, F. Heβberger, K. Hirose, H. Ikezoe, J. Khuyagbaatar, B. Kindler, B. Lommel, H. Makii, I. Nishinaka, T. Ohtsuki, S. Pain, R. Sagaidak, I. Tsekhanovich, M. Venhart, Y. Wakabayashi *et al.*, Phys. Lett. B **748**, 89 (2015).

[75] E. Prasad, D. J. Hinde, M. Dasgupta, D. Y. Jeung, A. C. Berriman, B. M. A. Swinton-Bland, C. Simenel, E. C. Simpson, R. Bernard, E. Williams, K. J. Cook, D. C. Rafferty, C. Sengupta, J. F. Smith, K. Vo-Phuoc, and J. Walshe, Phys. Lett. B **811**, 135941 (2020).

[76] B. M. A. Swinton-Bland, M. A. Stoyer, A. C. Berriman, D. J. Hinde, C. Simenel, J. Buete, T. Tanaka, K. Banerjee, L. T. Bezzina, I. P. Carter, K. J. Cook, M. Dasgupta, D. Y. Jeung, C. Sengupta, E. C. Simpson, and K. Vo-Phuoc, Phys. Rev. C **102**, 054611 (2020).

[77] K. Mahata, C. Schmitt, S. Gupta, A. Shrivastava, G. Scamps, and K.-H. Schmidt, Phys. Lett. B **825**, 136859 (2022).

[78] K.-H. Schmidt, B. Jurado, C. Amouroux, and C. Schmitt, Nucl. Data Sheets **131**, 107 (2016).

[79] D. J. Hinde, R. J. Charity, G. S. Foote, J. R. Leigh, J. O. Newton, S. Ogaza, and A. Chattejee, Nucl. Phys. A **452**, 550 (1986).

[80] D. J. Hinde, H. Ogata, M. Tanaka, T. Shimoda, N. Takahashi, A. Shinohara, S. Wakamatsu, K. Katori, and H. Okamura, Phys. Rev. C **39**, 2268 (1989).

[81] J. P. Lestone, Phys. Rev. Lett. **70**, 2245 (1993).

[82] J. P. Lestone and S. G. McCalla, Phys. Rev. C **79**, 044611 (2009).

[83] A. C. Berriman, D. J. Hinde, D. Y. Jeung, M. Dasgupta, H. Haba, T. Tanaka, K. Banerjee, T. Banerjee, L. T. Bezzina, J. Buete, K. J. Cook, S. Parker-Steele, C. Sengupta, C. Simenel, E. C. Simpson, M. A. Stoyer, B. M. A. Swinton-Bland, and E. Williams, Phys. Rev. C **105**, 064614 (2022).